

Ab Initio Investigation of Collective Charge Excitations in MgB_2

Wei Ku¹, W.E. Pickett¹, R.T. Scalettar¹, and A.G. Eguiluz²

¹*Physics Department, University of California, Davis, CA 95616*

²*Department of Physics and Astronomy, The University of Tennessee, Knoxville, TN 37996-1200, and Solid State Division, Oak Ridge National Laboratory, Oak Ridge, TN 37831-6030*

A sharp collective charge excitation is predicted in MgB_2 at $\sim 2.5\text{eV}$ for q perpendicular to the boron layers, based on an all-electron analysis of the dynamical density response within time-dependent density functional theory. This novel excitation, consisting of coherent charge fluctuation between Mg and B sheets, induces an abrupt plasma edge in the experimentally-observable reflectivity. The existence of this mode reflects the unique electronic structure of MgB_2 , that is also responsible for strong electron-phonon coupling. By contrast, the acoustic plasmon, recently suggested to explain the high T_c , is not realized when realistic transition strengths are incorporated.

PACS numbers: 74.70.Ad, 78.20.Bh, 78.20.-e

The high critical temperature, $T_c \sim 40\text{K}$, of the newly discovered [1] conventional superconductor MgB_2 has attracted much attention [2–9]. A consistent picture within BCS theory [10–12] seems to be given by the qualitative analysis [2,3] based on the large hole density of states at the Fermi surface, provided by the boron σ -bands. On the other hand, other possible contributions to pairing [7,8,13] have not been totally ruled out, since a quantitative analysis of T_c , via realistic treatment of screened electron-electron and electron-phonon interactions [4], has yet to be performed. The insight into the behavior of the cuprate superconductors resulting from consideration of the spin susceptibility suggests that it might be especially interesting to examine the possibility of unusual collective charge excitations in MgB_2 with such realistic treatments. In particular, a calculation of the dynamical density response would give detailed information on electronic excitations, which control most of the macroscopic properties, including the dielectric function and thereby superconductivity [12].

Even within phonon-mediated theories, there currently exists large speculation of the value of the Coulomb pseudopotential μ^* , from 0.02 to 1 [5,6]. An intriguing proposal [5] has recently suggested that an anomalously small μ^* may originate from the existence of an acoustic plasmon (AP) [14,15], which develops from two characteristic charge carriers in MgB_2 : (heavy) holes of B σ -bands and (light) electrons and holes of B π -bands. This is an important issue, as the existence of an AP can drastically alter the dynamical electronic screening and may even provide an additional pairing channel [15]. Thus, it is vital to re-examine the existing tight-binding result via a more realistic investigation that takes effects of the crystal potential fully into account.

In this Letter we present results of an *ab initio*, all-electron, calculation of the dynamical density-response function of MgB_2 within the framework of time-dependent density functional theory (TDDFT) [16]. Our key result is the prediction of a sharp collective mode

whose origin is the strong coherent charge fluctuation between parallel sheets of B and Mg. This novel charge excitation, found to reside within the [0002] zone-boundary gap, embodies a remarkable signature of the electronic structure of MgB_2 , and results in a dramatic change in the reflectivity near 2.5eV for q perpendicular to the boron layers. It also explains naturally the strong increase in the Raman efficiency reported very recently [9]. The impact of this mode on the Coulomb pseudopotential will be briefly addressed. In addition, with the matrix elements that control the transition probability fully included, the recently proposed acoustic plasmon is not realized in our results, as a consequence of weak intraband transition of the “heavy carriers”. Finally, comments on the proposed two-band-type superconducting instabilities will be given to further illustrate the importance of including realistic transition strengths.

Within TDDFT, the dynamical density response function $\chi(\vec{x}, t; \vec{x}', t') = \delta\rho(\vec{x}, t)/\delta V_{ext}(\vec{x}', t')$ with density ρ and external potential V_{ext} , can be obtained through the following integral equation [16]:

$$\chi = \chi^{KS} + \chi^{KS}(v + f_{xc})\chi, \quad (1)$$

where $\chi^{KS}(\vec{x}, t; \vec{x}', t')$ is the response function for “non-interacting” Kohn-Sham electrons, $v(\vec{x} - \vec{x}')$ is the Coulomb interaction, and $f_{xc}(\vec{x}, t; \vec{x}', t') = \delta V_{xc}(\vec{x}, t)/\delta\rho(\vec{x}', t')$ accounts for dynamical exchange-correlation effects (where V_{xc} is the time-dependent exchange-correlation potential in TDDFT.) Working in Fourier space, χ^{KS} can be calculated with the Kohn-Sham eigenenergies, $\epsilon_{\vec{k},n}$ and the corresponding eigenstates, $|\vec{k}, n\rangle$, of the ground state [17]:

$$\chi_{\vec{G}, \vec{G}'}^{KS}(\vec{q}, \omega) = \frac{1}{V} \sum_{\vec{k}} \sum_{n, n'}^{BZ} \frac{f_{\vec{k}, n} - f_{\vec{k}+\vec{q}, n'}}{\epsilon_{\vec{k}, n} - \epsilon_{\vec{k}+\vec{q}, n'} + \hbar(\omega + i0^+)} \times \langle \vec{k}, n | e^{-i(\vec{q}+\vec{G}) \cdot \vec{x}} | \vec{k} + \vec{q}, n' \rangle \langle \vec{k} + \vec{q}, n' | e^{i(\vec{q}+\vec{G}') \cdot \vec{x}} | \vec{k}, n \rangle, \quad (2)$$

where \vec{G} is a vector of the reciprocal lattice, n is a band

index, the wave vectors \vec{k} and \vec{q} are in the first Brillouin zone, and V is the normalization volume. Equation (1) is then numerically solved as a matrix equation [18].

We stress that this formalism is rigorous. Even though a formal connection between the Kohn–Sham eigenenergies and the quasi-particle energies has not been established, the physical meaning of the Kohn–Sham band structure (including the empty states) is to be realized through its contribution to the density fluctuation in χ^{KS} . The only physical approximation introduced in this work is the functional form of $V_{xc}(\vec{x}, t)$, for which the adiabatic local density approximation (ALDA) [16] is chosen. Since only the long wavelength limit is of interest in the present work, we further drop f_{xc} from Eq. (1), as its strength (within ALDA) cannot compete with the singular Coulomb potential without sizable crystal local-field effects [18]. In this limit, the dielectric function $\epsilon = (1 + v\chi)^{-1}$ can be visualized directly from the single-particle transitions of the Kohn–Sham particles, with the relation $\epsilon = 1 - v\chi^{KS}$.

Numerically, in order to resolve the features in the narrow energy range where the AP may occur, the broadening parameter, commonly employed in place of 0^+ in Eq. (2), needs to be very small ($\sim 10\text{meV}$). This in turn requires a dense k -mesh, to carefully sample the momentum–energy phase space near the Fermi surface. The results presented in this work correspond to a uniform mesh of $20 \times 20 \times 60$. In addition, summing the narrow δ -functions is avoided by first evaluating Eq. (2) on the imaginary frequency axis, followed by analytic continuation via Padé approximants [19].

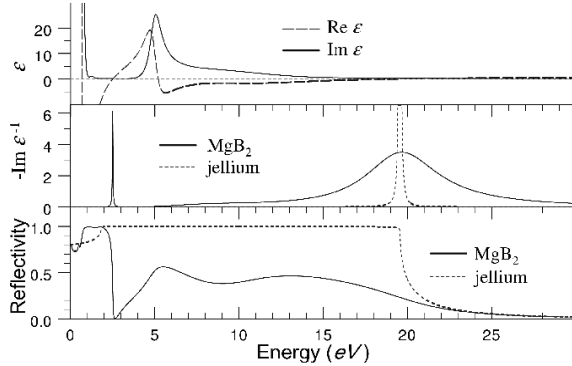


FIG. 1. Calculated dielectric function (upper panel), loss function (middle panel), and reflectivity (lower panel), as well as the jellium counterparts (dashed lines) for $q = 0.12\text{\AA}^{-1}$, along the c -axis.

The calculated dielectric function and corresponding loss function ($-\text{Im } \epsilon^{-1} = -v\text{Im } \chi$) along the c -axis, which should be directly probed by inelastic scattering experiments of electrons or x-rays [20], are shown over a broad energy range in Fig. 1. The wide structure [21] at $\omega \sim 20\text{eV}$ in the loss function is the conventional plasmon corresponding to density of ~ 8 electrons per unit

cell ($r_s \sim 1.8a_0$). It suffices to note the correspondence between the near vanishing of the dielectric function and the peak line shape of the loss function, illustrating the collective nature of this over-damped mode.

The most striking feature of the loss function shown in Fig. 1 is the sharp peak that occurs at $\sim 2.45\text{eV}$. The origin of this peak is evidently the prominent absorption at 5eV in $\text{Im } \epsilon$, whose physics will be addressed shortly. Indeed, the strength of this charge fluctuation (notice the vertical scale of ϵ) is large enough to generate, through screening, an additional zero in $\text{Re } \epsilon$ thereby inducing a new collective mode. The extremely long lifetime ($\Delta\omega < 10\text{meV}$) of this mode is a consequence of both the strong dynamical screening in the vicinity of its energy, as reflected in the large slope of $\text{Re } \epsilon$ [19,22], and the lack of particle–hole decay channels, courtesy of the large energy gap to be discussed below.

This additional collective excitation has a dramatic physical impact on the reflectivity, as shown in the bottom panel of Fig. 1. When possessing enough energy to excite this mode, the incident light suddenly penetrates the surface of the material with no reflection, much more abruptly than the case of normal metal (or jellium) with a plasmon. Consequently, this behavior greatly narrows the frequency range (from 20eV to 2eV) in which MgB₂ would look shiny. (The low-energy notches of both curves in the reflectivity would be absent in the optical limit.)

The existence of this mode also provides an obvious explanation for the strong resonance effect seen recently [9] in a 2.41eV (vs. 1.95eV) Raman scattering study of the E_{2g} phonon, since it is fluctuations in χ that give rise to Raman scattering. (The frequency dependence of the Raman efficiency is exactly that of χ [23]).

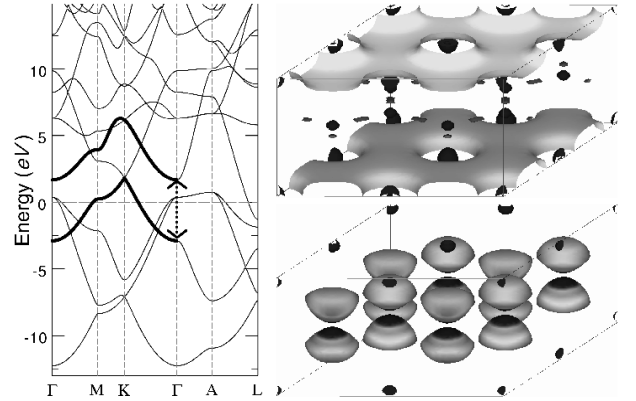


FIG. 2. Calculated band structure and density. The arrows in the band structure (left panel) indicate the large 5eV gap between parallel bands. The isosurfaces of density for states marked by the upper/lower arrows are shown in the upper/lower right panel, which contains $2 \times 2 \times 1$ unit cells with Mg in the corners.

Examination of the band structure, shown in the left panel of Fig. 2, reveals that the 5eV structure in $\text{Im } \epsilon$

originates mainly from the interband transitions between parallel bands. These transitions are facilitated by the strong [0002] crystal potential, which causes a large 5eV gap (indicated by the arrows) at the Γ point. Intriguingly, as shown in the right panel of Fig. 2, where the real-space charge distribution of states marked by the down and up arrows are illustrated, the states involved in the transitions reside in different planes and correspond to a B p_z π -state and a layered conducting state of Mg s -symmetry. Evidently, the above-mentioned additional mode consists of *coherent* charge fluctuations between B and Mg sheets, under the strong dynamical screening of low-energy intraband transitions. Note that since the physical origin of this additional mode is the periodic crystal potential [24] that gives the unique band structure of MgB₂, the same behavior would be totally absent if a homogeneous electron gas were assumed.

The wave vector dependence of the new collective mode, controlled by the competition between dynamical intraband screening and interband charge fluctuation, is shown in Fig. 3, in which the surface illustrates underlying single-particle transitions given by $\text{Im} \epsilon(q/[0001], \omega)$. The first branch at $\omega \sim 0.5\text{eV}$ of the low-energy ridge of the surface corresponds to the intraband charge fluctuation of the heavy carriers ($p_{x,y}$ σ -bands) to be discussed below, and the second branch to the light carrier (p_z π -bands), while the high-energy ridge demonstrates the 5eV interband transition. In the valley between these two main structures, where the phase space for single-particle excitation is closed due to the [0002] crystal potential, lies the weakly dispersed, induced collective mode (marked by dots), which eventually decays into electron-hole pairs of the light carriers at $q \sim 0.6\text{\AA}^{-1}$.

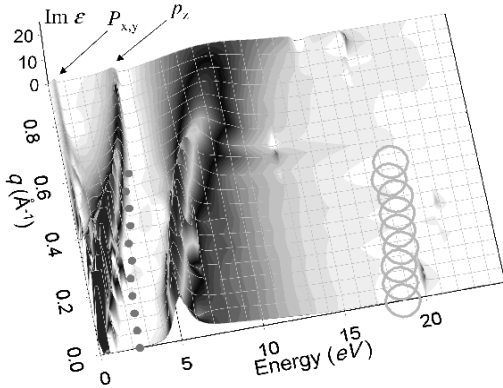


FIG. 3. Dispersion of collective modes and the single-particle decay channel. The dispersion of the induced/nominal collective mode is denoted by dots/circles until it becomes difficult to identify the peak energy of the plasmon. The surface illustrates $\text{Im} \epsilon(q, \omega)$ for $\vec{q}/[0001]$.

It is natural to wonder about the impact of this additional mode on the superconductivity, through reduction of the Coulomb pseudopotential, μ^* . Within the static

approximation adopted by previous authors [11,12], this new mode is found to have almost no effect on the static screened interaction, due to its very sharp line shape and small spectral weight compared to the conventional plasmon. In fact, the static limit of our resulting screened interaction is almost identical to that obtained from the homogeneous electron gas, despite its highly anisotropic energy dependence. It is possible to evaluate μ^* from the screened interaction [25] obtained in this work. However, because of the highly anisotropic nature of the Fermi surfaces, even the very idea of treating the screening through a single Coulomb pseudopotential may not be adequate (c.f. Eq. (2.26) of Ref. [12]).

Now we address the proposed [5] AP with calculated dielectric function for small momentum/energy, shown in Fig. 4. The two main peak structures in $\text{Im} \epsilon$ are related to the unusual characteristic of the Fermi surface [3]. The peak of lower energy corresponds to the intraband charge fluctuation of the heavy carriers, while the main peak results from the light carriers. More specifically, for a small momentum transfer q along the c -axis, the cylindrical $p_{x,y}$ σ -hole Fermi surfaces [3] contribute to smaller energy (heavier mass), compared to the two-dimensional, tubular p_z π -hole and π -electron Fermi surfaces. This double-peak structure is precisely what led to the suggestion of AP [5], as the plasmon energy of the heavy carriers might be greatly screened by the light carriers and reduced to the upper edge of low-energy peak, whose energy increases linearly with small q .

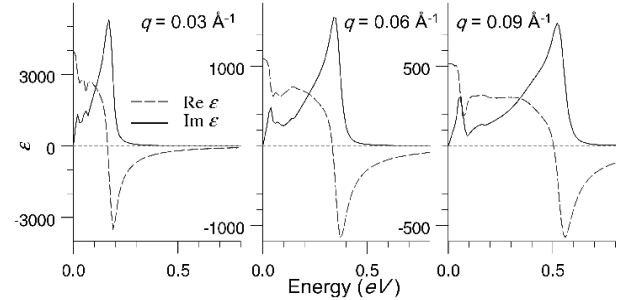


FIG. 4. Calculated dielectric function of MgB₂, for small q 's along the c -axis. The low/high-energy peaks of $\text{Im} \epsilon$ correspond to charge fluctuation of the heavy/light carriers. Note the large difference in the spectral weight and that $\text{Re} \epsilon \gg 1$ between these two main structures.

However, this simple picture neglects electron-hole decay channels and the relative strength (or spectral weight) of these two carriers. As shown in Figure 4, for small q there is a large supply of charge fluctuations ($\text{Im} \epsilon \gg 1$) involving the light carriers at the upper edge of the low-energy peak. As a result, any collective mode of this energy would rapidly decay into electron-hole pairs (Landau damping) and have a negligible lifetime. In fact, our analysis suggests that a gap in the light-carrier bands at the Fermi energy is needed to allow

an AP to exist. Furthermore, in this energy range, $\text{Re}\epsilon$ is considerably larger than unity, reflecting the fact that the spectral weight from the heavy carriers is insignificant compared to the strength of the screening from the light carriers. In short, the potential acoustic plasmon is totally screened out and should not contribute to μ^* .

This kind of interplay between these two structures cannot be faithfully estimated by just counting the phase space, as performed in Ref. [5] with parameterized tight-binding bands. Instead, a careful evaluation of the corresponding transition probability, controlled by the matrix elements in Eq. (2), is necessary. The commonly made approximation of unit probability (from assuming jellium wave functions) risks promoting unphysical charge fluctuations in the calculation, especially in the case of multi-band models [26].

For a similar reason, the recently proposed two-band-type superconducting instability [7] in MgB_2 is also not supported by our results. For $q \sim (0, 0, \pi/c)$, where the nesting between B π -electron and π -hole Fermi surfaces becomes “perfect”, there is no apparent enhancement at zero energy in our dielectric functions ($q \sim 0.9\text{\AA}^{-1}$ in Fig. 3), contrary to the large interband polarizability obtained in Ref. [7]. Even though the formalism adapted in this work is different from that in Ref. [7], based on the experience gathered in the past years [19,27], we are confident that our results should not suffer from qualitative error for a simple sp system like MgB_2 . Thus, the enhancement of interband pair scattering in Ref. [7] is an artifact of omitting the transition probability (c.f. Eq. (9) of Ref. [7]) as discussed above.

In conclusion, a novel sharp collective mode, involving coherent charge fluctuation between B and Mg sheets, is predicted. This additional collective mode has a great impact on the optical properties of the material – suddenly switching off the reflectivity in the corresponding energy. It also naturally explains the strong increase in the reported Raman efficiency at 2.41eV . By contrast, the recently suggested AP is not supported by careful evaluation of the dynamical density response functions, with the full information of all-electron Kohn-Sham band structure. The weak charge fluctuation from heavy carriers is totally screened out by the light carriers. Thus, AP is effectively ruled out as a possible mechanism that brings an anomalously small Coulomb pseudopotential, μ^* . Our results further demonstrate the importance of inclusion of realistic crystal potential effects, through the band dispersions (gaps) and matrix elements, in the calculation of charge fluctuation for systems with non-trivial (non-spherical) Fermi surfaces.

This work was supported by DOE Grant DE-FG03-01ER45876 and an Accelerated Strategic Computing Initiative grant through Lawrence Livermore National Laboratory. A.G.E. and R.T.S. acknowledge support from NSF and NERSC.

- [1] J. Nagamatsu *et al.*, Nature 410, 63 (2001).
- [2] J. M. An and W. E. Pickett, Phys. Rev. Lett. 86, 4366 (2001).
- [3] J. Kortus *et al.*, Phys. Rev. Lett. 86, 4656 (2001); S.V. Shulga *et al.*, cond-mat/0103154; T.A. Callcott *et al.*, cond-mat/0103593.
- [4] Y. Kong *et al.*, cond-mat/0102499; S. Haas and K. Maki, cond-mat/0104207; P. Ravindran *et al.*, cond-mat/0104253; A.Y. Liu *et al.*, cond-mat/0103570.
- [5] K. Voelker *et al.*, cond-mat/0103082.
- [6] A.S. Alexandrov, cond-mat/0104413.
- [7] K. Yamaji, cond-mat/0103431.
- [8] S.L. Bud’ko *et al.*, Phys. Rev. Lett. 86, 1877 (2001); M. Imada, cond-mat/0103006; N. Kristoffel and T. Ord, cond-mat/0103536.
- [9] H. Martinho *et al.*, cond-mat/0105204.
- [10] J. Bardeen *et al.*, Phys. Rev. 108, 1175 (1957).
- [11] G.M. Eliashberg, Zh. Eksperim. I Teor. Fiz. 38, 966 (1960); P.B. Allen and R.C. Dynes, Phys. Rev. B 12, 905 (1975).
- [12] D.J. Scalapino *et al.*, Phys. Rev. 148, 263 (1966).
- [13] N.E. Bickers *et al.*, Int. J. Mod. Phys. B 1, 687 (1987).
- [14] D. Pines, Can. J. Phys. 34, 1379 (1956); B.N. Ganguly and R.F. Wood, Phys. Rev. Lett. 28, 681 (1972); J. Ihm *et al.*, Phys. Rev. B 23, 3258 (1981); G.S. Canright and G. Vignale, Phys. Rev. B 39, 2740 (1989); G.D. Mahan and Ji-Wei Wu, Phys. Rev. B, 39 265 (1989).
- [15] H. Fröhlich, J. Phys. C 1, 544 (1968).
- [16] M. Petersilka *et al.*, Phys. Rev. Lett. 76, 1212 (1996).
- [17] P. Blaha *et al.*, WIEN97.8, Technical University of Vienna, 1997; J.P. Perdew and Y. Wang, Phys. Rev. B 45, 13244 (1992).
- [18] The off-diagonal matrix elements in Eq. (2) incorporate the “crystal-local fields”, whose effect turns out to play a minor role in the present work.
- [19] Wei Ku and A.G. Eguluz, Phys. Rev. Lett. 82, 2350 (1999) and references therein.
- [20] J. Fink, *Unoccupied Electronic States*, edited by J. C. Fuggle and J. E. Inglesfield (Springer, Berlin, 1992), p.203; J. P. Hill *et al.*, Phys. Rev. Lett. 77, 3665 (1996).
- [21] Fine structures in the actual line shape (e.g. a dip in the center of the plasmon peak) are suppressed for the ease of visualization.
- [22] K. Sturm and L.E. Oliveira, Phys. Rev. B 24, 3054 (1981).
- [23] M. Cardona, Physica C 318, 30 (1999).
- [24] This additional mode can also be interpreted roughly as “zone-boundary collective state” if that concept is extended to cases with ionic anisotropic bonds; K. Sturm and L.E. Oliveira, Phys. Rev. B 30, 4351 (1984).
- [25] K.-H. Lee *et al.*, Phys. Rev. B 52, 1425 (1995).
- [26] Our work employs no pseudopotential which may introduce inaccuracy in evaluating the matrix elements. B. Adolph *et al.*, Phys. Rev. B 63, 125108 (2001); J.M. Sullivan and A.G. Eguluz (to be published).
- [27] A.G. Eguluz, Wei Ku and J.M. Sullivan, J. Phys. Chem. Solids 61, 383 (2000); A.A. Quong and A.G. Eguluz, Phys. Rev. Lett. 70, 3955 (1993); N.E. Maddocks *et al.*, Europhys. Lett. 27, 681 (1994); F. Aryasetiawan and O. Gunnarsson, Phys. Rev. Lett. 74, 3221 (1995).